Gauging extreme floods on YouTube: Application of LSPIV to home movies for the post-event determination of stream discharges

R. Le Boursicaud, Lionel Pénard, A. Hauet, F. Thollet, J. Le Coz

Author-produced version of the article published in Hydrological Processes (2016), Volume 30, Issue 1, p 90–105
The original publication is available at http://onlinelibrary.wiley.com DOI: 10.1002/hyp.10532

Gauging extreme floods on YouTube: Application of LSPIV to home movies for the post-event determination of stream discharges

Running head: Application of LSPIV to flood home movies

R. Le Boursicaud[1], L. Pénard[1], A. Hauet[2], F. Thollet[1], J. Le Coz[1]

Correspondence to J. Le Coz, e-mail: jerome.lecoz@irstea.fr

1. Irstea, UR HHLY, Hydrology-Hydraulics, 5 rue de la Doua CS70077, 69626 Villeurbanne cedex, France

2. EDF-DTG, 21 avenue de l'Europe BP41, 38040 Grenoble cedex 09, France

Abstract

Movies taken by witnesses of extreme flood events are increasingly available on video sharing websites. They potentially provide highly valuable information on flow velocities and hydraulic processes that can help improve the post-flood determination of discharges in streams and flooded areas. We investigated the troubles and potential of applying the now mature LSPIV technique to such flood movies that are recorded under non-ideal conditions. Processing was performed using user-friendly, free software only, such as Fudaa-LSPIV. Typical issues related to the image processing and to the hydrological analysis are illustrated using a selected example of a pulsed flash-flood flow filmed in a mountainous torrent. Simple corrections for lens distortion (fisheye) and limited incoherent camera movement (shake) were successfully applied and the related errors were reduced to a few percents. Testing the different image resolution levels offered by YouTube showed that the difference in time-averaged longitudinal velocity was less than 5% compared to full resolution. A limited number of GRPs, typically 10, is required but they must be adequately distributed around the area of interest. The indirect determination of the water level is the main source of uncertainty in the results, usually much more than errors due to the longitudinal slope and waviness of the flow free-surface. The image-based method yielded direct discharge estimates of the base flow between pulses, of the pulse waves, and of the time-averaged flow over a movie sequence including a series of 5 pulses. A comparison with traditional indirect determination methods showed that the critical-depth method may produce significantly biased results for such a fast, unsteady flow, while the

Author-produced version of the article published in Hydrological Processes (2016), Volume 30, Issue 1, p 90–105
The original publication is available at http://onlinelibrary.wiley.com DOI: 10.1002/hyp.10532

slope-area method seems to be more robust but would overestimate the time-averaged flow rate if applied to the high-water marks of a pulsed flow.

Keywords: hydrometry; flood; LSPIV; discharge; home movie; video sharing website

Author-produced version of the article published in Hydrological Processes (2016), Volume 30, Issue 1, p 90–105
The original publication is available at http://onlinelibrary.wiley.com DOI: 10.1002/hyp.10532

1 Introduction

1.1 Large uncertainties in indirect post-flood discharge estimates

The accurate knowledge of river discharge during extreme flood events is key for most studies of the flood-related hydrological processes. Very often, flood discharge measurements are lacking because of a range of technical limitations in streamgauging field operations. It often happens that deploying the instruments was too dangerous or too uncertain because of free-surface conditions, drag, floating debris, high suspended-load or moving bed. It also happens that the hydrometry staff cannot get to the gauging site when the flood wave was too sudden and too short or when roads and access are flooded. Last, discharge measurements may be lacking simply because discharge estimates are requested at a site where a hydrometric station did not exist or was destroyed by high flows. In such common situations, a post-flood analysis is required in order to support the indirect determination of peak discharge (WMO, 2010, chapter 9). The method is based on the field collection of all relevant information on the flow magnitude and dynamics, especially high-water marks, channel geometry and roughness, control section geometry, etc. The aim is to feed conventional hydraulic formulations related to a channel control (slope-area method) using the Manning-Strickler equation, to different types of critical section controls (flow over dams and weirs, through culverts, at width contractions), or to other hydraulic properties such as free-surface superelevation in bends.

The uncertainty of indirect discharge estimates is usually much larger than the uncertainty of discharge measurements from streamgauging or stage-discharge relations calibrated at hydrometric stations. Jarrett (1987) showed that the slope-area method can typically lead to 100% overestimation of flood discharges in mountain rivers where the critical-depth method is preferable. Lumbroso and Gaume (2012) highlighted the difficult estimation of reliable Manning's n flow resistance coefficients, especially for supercritical flows. Amongst major sources of error are the uncertainty of high-water marks and derived longitudinal slope, the questionable applicability of hydraulic formulas established for ideal conditions, the unobserved scour and deposition processes during the flood (Kirby, 1987; Gaume et al., 2004). A major issue in the indirect discharge determination is the absence of flow velocity measurements.

Borga et al. (2008) also insist on the limited spatio-temporal resolution of indirect peak discharge es-

Author-produced version of the article published in Hydrological Processes (2016), Volume 30, Issue 1, p 90–105
The original publication is available at http://onlinelibrary.wiley.com DOI: 10.1002/hyp.10532

timates: the post-flood analysis aims at reconstructing the flood event dynamics at a synoptic scale. Beyond the collection of hydraulic data, the post-flood field survey usually offers the opportunity of interviewing eyewitnesses, which may provide valuable, though variably uncertain information on the flood dynamics and morphodynamical processes (Gaume and Borga, 2008). They also often provide additional material such as pictures and movies: Lumbroso and Gaume (2012) recommend to use them to check the consistency of velocity estimates greater than 3 m/s, either from the displacement of visible flow tracers or from the height of flow superelevation against an obstacle.

Numerical simulation can also be used to investigate the hydrological response of the catchment and the stage-discharge relation along the river network: for instance, Bonnifait et al. (2009) successfully combined distributed hydrological and hydraulic modelling to reconstruct the 2002 flash-flood event in the Gard river catchment based on the post-flood analysis conducted by Delrieu et al. (2005). However, even the best numerical simulation cannot compensate for the scarcity and large uncertainty of post-flood flow velocity and discharge estimates.

1.2 Potential of LSPIV for post-flood analysis

Since floods are important events for the people living in the vicinity of the impacted rivers, witnesses often take pictures or record videos of those events. The fast-growing development of digital imaging technologies allows non-professional people to record high quality videos. Sharing videos in the Internet is nowadays very common, especially for videos of extreme natural events. As a consequence, each recent flood occurring in inhabited areas has its hundreds or thousands of videos in the Internet. As an example, searching "Flood Boulder 2013" and "Flood Brisbane 2011" on YouTube yields 65 000 and 43 000 results, respectively.

A simple look at those videos can bring a lot of information about the flow processes: how high was the water, how extended were the flooded areas, what kind of obstacles were opposed to the flow, what kind of objects were put in motion, or what was roughly the velocity and direction of the water. In this paper, we investigate the capability of calculating quantitative hydraulic data, such as water height, flow velocity and eventually discharge from home movies taken by flood witnesses. Image-based methods can indeed be used for the calculation of hydraulic parameters. The first

Author-produced version of the article published in Hydrological Processes (2016), Volume 30, Issue 1, p 90–105
The original publication is available at http://onlinelibrary.wiley.com DOI: 10.1002/hyp.10532

image-based velocimetry technique was developed for laboratory applications in the 1960's and called PIV for Particle Image Velocimetry (Adrian, 1991). In the following decades, different image analysis techniques were developed, such as the Particle Tracking Velocimetry PTV (Perkins and Hunt, 1989; Lloyd et al., 1995), the Large-Scale Particle Image Velocimetry (LSPIV, Fujita et al., 1998), or the Space-Time Image Velocimetry STIV (Fujita et al., 2007). Among those methods, LSPIV was chosen as a tool for the present study because it is currently the most mature and widely available image-based velocimetry technique.

The efficiency of LSPIV for measuring free-surface velocities and discharge in rivers for flood conditions has been recurrently demonstrated since the proof-of-concept application by Creutin et al. (2003). Flood discharges were successfully computed using images produced by commercial video cameras mounted on mobile systems (Kim et al., 2008; Le Coz et al., 2010; Dramais et al., 2011), LSPIV-dedicated video stations (Hauet et al., 2008a; Le Coz et al., 2010), existing video monitoring (CCTV) system (Tsubaki et al., 2011) or even helicopter-borne cameras (Fujita and Hino, 2003; Fujita and Kunita, 2011).

Muste et al. (2011) proposed a detailed review of the LSPIV technique. Basically, LSPIV entails three major steps :

- recording of a sequence of images, knowing the time interval, δt, between two images in a pair;
- orthorectification of the images, in order to correct perspective distortion effects and to georeference pixels. This geometrical correction of the pictures is usually achieved through a 3D plan-to-plan perspective projection calibrated with Ground Reference Points (GRP) (Jodeau et al., 2008);
- statistical analysis applied to each pair of orthorectified images to determine the displacement of natural or artificial tracers of the free surface flow such as boils, surface ripples, vegetation debris, etc. At each node of the computational grid, cross-correlation is applied to 256-level gray-scale square interrogation areas with a sub-pixel optimisation. More details about the data processing and the limitations of the technique can be found in Le Coz et al. (2014).

The LSPIV analysis provides instantaneous 2-D velocity fields of the free surface velocities. Knowing

Author-produced version of the article published in Hydrological Processes (2016), Volume 30, Issue 1, p 90–105
The original publication is available at http://onlinelibrary.wiley.com DOI: 10.1002/hyp.10532

the bathymetry of a cross-sectional transect and modelling the vertical velocity distribution lead to an estimation of the river discharge.

In a review of previous works on LSPIV accuracy, Muste et al. (2008) reported an average total error in velocity of 10% and maximum error of 35%. Such numbers were supported by the consideration of 27 elemental error sources and the results of comparison to other velocimetry techniques taken as references, with observed differences ranging from 3.5% in ideal laboratory conditions to 10% or even 16% in field conditions. Though Muste et al. (2008) stated that the uncertainty in estimated discharge should be lower than the uncertainty in velocities, the former is actually difficult to predict from the latter. Typically, from comparison tests at their gauging station, Le Coz et al. (2010) estimated the uncertainty in velocity to be lower than 10% while the uncertainty in discharge was lower than 20% in good image conditions, but up to 30-80% in poor image conditions. Taking a well-established rating curve as a reference, Dramais et al. (2011) estimated their uncertainty in discharge to be as low as 10% for flow and image conditions similar to those of many flood home movies.

A complete uncertainty analysis method for flood discharge measurements using the conventional LSPIV technique is still missing, mainly because: orthorectification and LSPIV image processing involve complex error propagation; errors in velocity are varying spatially according to flow and image conditions; errors in discharge estimate are significantly affected by errors in water level estimate, cross-sectional geometry and assumptions on the unmeasured flow structure, which all are difficult to quantify under flood conditions in a natural stream. Hauet et al. (2008b) opened a promising way to conduct efficient sensitivity analysis using a numerical simulator that combined the river flow, the camera and the LSPIV processing. Nevertheless, LSPIV discharge uncertainty estimates from empirical studies are acceptably low to improve post-flood analysis results and the extension of stage-discharge rating curves to ungauged high flows.

1.3 Major issues related to the analysis of flood movies

In most cases flood movies are produced by non-professional witnesses in non controlled conditions with no velocimetric objective. Using such videos for LSPIV applications raises several issues that

Author-produced version of the article published in Hydrological Processes (2016), Volume 30, Issue 1, p 90–105
The original publication is available at http://onlinelibrary.wiley.com DOI: 10.1002/hyp.10532

have to be addressed.

The first point is to select from the available movies those that are eligible for LSPIV processing. Both river banks have to be visible in the image so that a complete cross-section is monitored. Another selection factor is that the flow should not be too wavy and non uniform, and the water surface has to be planar according to usual LSPIV hypotheses.

The second issue regards image processing. Traditional LSPIV sequences are captured with a known camera, so that usually focal length and distortion are either known or can be calibrated. The camera is placed at a known and steady position and all the necessary topography measurements are made in the field. Thus, the projection equations that relate ground and image reference systems can be determined and do not vary with time. In the case of home movies, the camera is unknown and hand-held, and parameters have to be estimated from the images. Automatic methods have been developed, such as self-calibration (Maybank and Faugeras, 1992) and motion estimation (Pollefeys et al., 2004), to overcome this problem.

The third point deals with the link between images and the scene. LSPIV velocity and discharge results are highly dependent on the water level, as noted by Dramais et al. (2011). In the case of home movies, this parameter has to be estimated directly from the images. Moreover, in order to perform the absolute image registration, GRPs have to be present within the images, ideally placed on both sides of the flow.

Finally, issues related to the properties of the flow and of the hydrological event are also raised by the application of LSPIV technique to flood movies recorded by witnesses. To calculate discharge from surface velocity estimates, the bathymetry of the reach has to be known and a realistic depth-average to surface velocity ratio, or 'velocity coefficient' has to be selected. A specific attention should be paid to mobile bed conditions and to the subsequent morphodynamical evolutions during the event, which may dramatically increase the uncertainty in the flow structure and in the wetted area, hence in the discharge estimate. Another difficulty is to determine the precise location, date and time of the movie relative to the whole hydrological event.

Author-produced version of the article published in Hydrological Processes (2016), Volume 30, Issue 1, p 90–105
The original publication is available at http://onlinelibrary.wiley.com DOI: 10.1002/hyp.10532

1.4 Objectives of this study

The scope of this methodological paper is to cover the main issues related to the application of the conventional LSPIV technique to flood home movies. Technical problems and solutions are illustrated using the same application example, a typical movie taken by the observer of a storm flood in a channelized torrent of the French Alps. The sensitivity of discharge estimates to the identified sources of errors is investigated. The specific issues related to the image processing of flood home movies are presented first. We eventually discuss the limitations and added value of the proposed method for the indirect determination of flood discharges, especially when pulsating flows occur.

2 Material and methods

2.1 Study case: A flash-flood in an alpine torrent

The study site is located in the French Alps in the Saint-Julien torrent at Saint-Julien-Mont-Denis, France. The catchment area of the river at the point where the video was recorded is about 20 km^2. The geographic coordinates at this point are 6°24'08.8" E / 45°15'26.1" N. The Saint-Julien torrent is a typical concrete-lined, steep mountain stream prone to flash flood. No hydrometric station is available in that stream.

The bed of the Saint-Julien torrent is entirely artificialized from 200 meters upstream of the study site, to the confluence with the Arc river 1.6 km downstream. The straight channel has a trapezoidal cross-section which is ∼5 m wide at the bottom. Banks are 45-degree slopped and made of concrete sealed riprap rocks, while the bottom is paved with rectangular concrete flagstones. One meter high steps were built every 20 m along the channel to reduce the local longitudinal slope. The area of interest of the recorded pictures includes a uniform section with a gradient of 0.063 m/m downstream of a step acting as a weir.

Beside periods of snow melting during Spring and occasional storm events with heavy precipitation, the stream has a very low, if not zero discharge, as is the case at the beginning of the studied video. Flash floods during Summer storms may form and propagate extremely rapidly. On the 22nd

Author-produced version of the article published in Hydrological Processes (2016), Volume 30, Issue 1, p 90–105
The original publication is available at http://onlinelibrary.wiley.com DOI: 10.1002/hyp.10532

(a) Measuring the cross-section of the main weir (b) Measuring a GRP on the flagstone edges

Figure 1: Views of the post-flood topography operations in the Saint-Julien torrent channel.

of August 2011, heavy precipitations resulted in a flash flood that lasted about 40 min. Such a hydrological event is not unusual in the torrential tributaries of the Arc river. The response of the Arc river was recorded at the Pontamafrey station located 10 km downstream of the junction with the Saint-Julien torrent. The peak discharge was very limited: 80 m^3/s, while the 2-year return period discharge is 260 m^3/s (cf. Dramais et al., 2011). However, the suspended load concentration (8.5 g/L at peak) and flux (7 t/s at peak, 31 000 t over the event) were significant.

As will be discussed later, the event is characterized by violent pseudo-periodic pulses that appear as translatory breaking waves with obviously much higher velocity and discharge than the quasi-steady base flow between those pulses. The water is almost black, which suggest that the suspended load is very high, likely higher than 50 g/L. Still, the flow seems to behave as a Newtonian fluid, except for the first dry front that pushes a lot of debris and rocks as a slug.

The complementary measurements necessary to the LSPIV analysis, such as topography, ground reference point coordinates, and the water level at different moments of the video were later performed by our staff (cf. Fig. 1). The topography survey was achieved using a total station (Leica TC305). Due to unavoidable alignment errors, the positioning uncertainty was estimated to be roughly ± 1 cm (within the 95% confidence level).

A reference transect for computing discharge was measured in the uniform reach downstream of the weir, which was also measured. The bottom width is equal to 5.1 m in the reference transect. It

Author-produced version of the article published in Hydrological Processes (2016), Volume 30, Issue 1, p 90–105
The original publication is available at http://onlinelibrary.wiley.com DOI: 10.1002/hyp.10532

can be seen in Fig. 1 that bedload transport produced limited deposits in the recorded reach and likely led to negligible changes in the cross-section area during the event.

2.2 Study case: Images and camera

The event was captured by Alexandre Modesto, a local flash-flood enthusiast who posted a montage of the video online[1] and further authorized us to use his film for research purpose. The recording starts before the arrival of the flash flood, showing the geometrical pavement of the dry bed, as visible in Fig. 2(a). The stream is filmed from a bridge facing upstream, at a 1920×1080 pixels resolution and a 25 frames per second sampling rate, using a Canon EOS 5D mark II with a 16 mm fisheye Zenitar lens. The fisheye lens produces a large amount of distortion. Besides, due to the absence of a tripod during the recording, the video presents a typical camera shake.

This flood home movie was chosen to illustrate this paper because of three main advantages. Firstly, the author is identified, which opened the possibility to have access to the full resolution original video and to get informations on the hydrological event. Secondly, the hydrological event itself is of great interest, especially for the study of the pseudo-periodic pulses. Finally, the recording starts before the arrival of the water flow and the presence of a regular grid on the dry bed is a key point for image processing tests such as distortion removal, or impact of slope correction.

The selected movie is not particularly favourable to the application of LSPIV, at least because of camera movements, wide-angle lens distortion, scarce fixed reference points in a semi-urban environment and streamwise shooting along an inclined flow in a steep channel. It is therefore useful to investigate the errors related to these frequent limitations of flood home movies. The main favourable property of this study case is that the channel geometry is almost perfectly known since the bed is concrete-lined and bedload deposits are clearly negligible (cf. Fig. 1). In many other cases in natural, alluvial streams, possible bed evolutions during the flood are a major source of uncertainty in the discharge estimates.

The studied flood home movie lasts for more than 17 minutes. A reference sequence of 50 images was selected, starting at time 5:00. All the image processing and LSPIV analyses were performed on this reference sequence (cf. sections 3.2, 3.3, 3.4, 3.5 and 4.2), except the larger movement in section

[1] http://www.youtube.com/watch?v=V1H7V90o8JY

Author-produced version of the article published in Hydrological Processes (2016), Volume 30, Issue 1, p 90–105
The original publication is available at http://onlinelibrary.wiley.com DOI: 10.1002/hyp.10532

3.3 for which a specific sequence was required (time 7:27), and the pulse flow analysis detailed in section 4.4. Additionally, an image of the beginning of the video when the torrent bed is still dry is used for the geometric evaluation of the orthorectification step (cf. section 3.1).

LSPIV parameters were kept constant for all the tests presented in this paper. The time interval δt between consecutive frames sampled from the original movie is equal to 0.04 s. The resolution of the orthoimages was set to 0.03 m/pixel. The size of the interrogation area (IA), i.e. the square image pattern on which correlation is computed, is 30 pixels. The extent of the search area (SA), i.e. the rectangle within which the center of the IA is positioned to compute all the investigated correlation coefficients, is 25 pixels, 0 pixels and 15 pixels in the downstream, upstream and spanwise directions, respectively. No data screening was applied to the obtained velocity vectors.

2.3 A free software approach for a reproducible method

For this study, the LSPIV analysis was conducted using Fudaa-LSPIV, a free software available online[2] that uses the Fudaa libraries released under the GPL licence (Le Coz et al., 2014). Fudaa-LSPIV is a user-friendly Java graphical user interface that calls Fortran routines to import and process sequences of grayscale PGM images extracted from movies, passing through all the steps that are required for a LSPIV analysis of velocity fields, other derived hydrodynamic quantities, and discharge.

Image preprocessing steps are performed by two free open-source software tools. AvConv[3] is a video and audio converter. It is used for frame extraction from video files. Hugin[4] was initially designed for panorama switching. It contains all image processing functions needed for distortion correction and image alignment.

As such, the method described in this paper is fully reproducible by any reasonably skilled reader who would be willing to study similar flood home movies. The presented study case is also reproducible since all the necessary parameters are provided in this paper, the raw video material is available on YouTube and the Fudaa-LSPIV zip file containing the reference image sequence,

[2] https://forge.irstea.fr/projects/fudaa-lspiv/files
[3] https://www.libav.org
[4] http://hugin.sourceforge.net

Author-produced version of the article published in Hydrological Processes (2016), Volume 30, Issue 1, p 90–105
The original publication is available at http://onlinelibrary.wiley.com DOI: 10.1002/hyp.10532

computational parameters and topography data is provided as online additional materials.

3 Image processing issues

In this section, two different kinds of image processing issues are addressed. Some issues are strictly specific to flood home movies: Creation of undistorted images; Image alignment; Impact of image resolution. On the other hand, issues dealing with the selection of GRPs and longitudinal slope correction are not specific to home movies only and may be needed for all LSPIV image sequences. The investigation of such error sources is important for home movies since the field is unknown a priori, and fieldwork is particularly costly.

3.1 Creation of undistorted images

Home movies are captured by uncalibrated sensors whose internal parameters are unknown. Since the LSPIV technique was originally developed for calibrated perspective cameras, its direct applicability to this type of images was questionable. A first processing step is therefore introduced to remove distortion from the images. In the case under study , the camera that acquired the images has a fisheye lens, which induces a large amount of barrel distortion (cf. Fig. 2(a)). Since the LSPIV technique was originally developed for perspective cameras, its direct applicability to this type of images was uncertain. On the one hand, the image projection equations used for orthorectification are not valid anymore, calling for distortion correction. On the other hand, the area of interest in the image is located near the image center, where the distortion effect is minimal. In order to estimate the impact of distortion on LSPIV results, we performed the whole LSPIV process with both the original images and the geometrically corrected images.

Distortion correction was conducted with Hugin. A rectilinear image was created by Hugin from the original fisheye image. The only parameter of this transformation is the focal length (16 mm). The corrected image is presented in Fig. 2(b). It can be seen that formerly bended lines are straightened, e.g. the bridge guardrail in the foreground or the edges of the rectangular stones paving the torrent bottom. The images were then orthorectified in the torrent bottom plane. Orthoimages were created by Fudaa-LSPIV, based on the transformation from image to field coordinates of the GRPs

Author-produced version of the article published in Hydrological Processes (2016), Volume 30, Issue 1, p 90–105
The original publication is available at http://onlinelibrary.wiley.com DOI: 10.1002/hyp.10532

(Le Coz et al., 2014). Nine GRPs were used in the rectilinear case. In the fisheye case, 2 GRPs were discarded because they lie far away from the image center and their distortion values were too large to perform registration with Fudaa-LSPIV.

The results of this orthorectification step are given in Fig. 2(c) and Fig. 2(d). The actual size of the flagstones paving the torrent bottom is 1 m $\times$ 0.5 m. In the rectilinear orthorectified image, linear structures are correctly represented and the obtained stone size fits the measurements. In contrast, in the fisheye case, the bottom pavement is distorted with barrel distortion still present in the image and the pavement size is not uniform. Moreover, the measured lengths of the paving stones within the area of interest surrounding the reference cross-section range from 15% to 23% above the actual value. In this study case, the distortion due to the fisheye lens makes the LSPIV results significantly biased without the correction step. However, in many usual cases, lens distortion remains low around the image center with negligible effects on LSPIV results.

3.2 Selection of the Ground Reference Points (GRPs)

The selection of Ground Reference Points is a mandatory step in the LSPIV process. Typically, Le Coz et al. (2010) like many others used artificial targets to identify GRPs in their experimental set-up. In the case of flood home movies, the selection of GRPs is achieved afterwards, using visible, fixed elements of the river environment as targets. The number of available targets and their spatial distribution may vary greatly from one video to another, which would be less true in the case of a fixed LSPIV station or of professional LSPIV streamgauging. In the presented case study, the 3-D coordinates of 14 points were measured during a post-event field survey, 9 of which are clearly identified in the image sequence even when the channel is flooded. Those 9 GRPs are reported in Fig. 2(b).

The issue is to determine the number of GRPs required to register the images along with their optimal arrangement in the image. According to the LSPIV theory (see Muste et al., 2010), a minimum of 6 GRPs are required since there are 11 unknowns and each GRP brings 2 equations. Moreover, the GRPs should surround the area of interest and not be aligned.

Fig. 3 shows the impact of the number and location of GRPs on the surface velocity field. In Fig. 3(a)

Author-produced version of the article published in Hydrological Processes (2016), Volume 30, Issue 1, p 90–105
The original publication is available at http://onlinelibrary.wiley.com DOI: 10.1002/hyp.10532

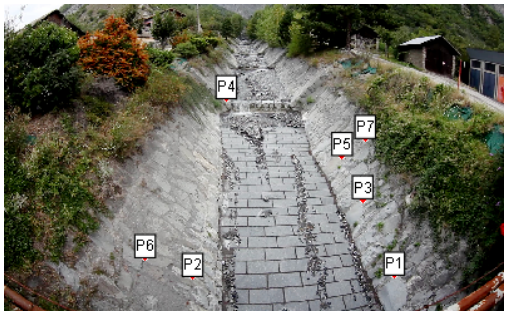

(a) Original fisheye image

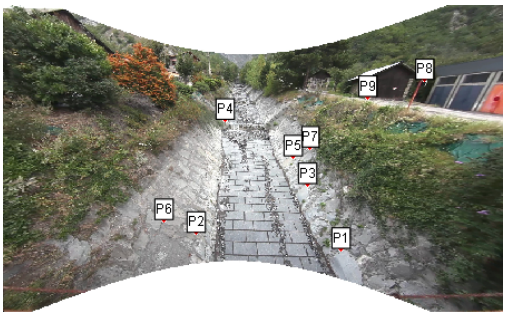

(b) Rectilinear transformed image

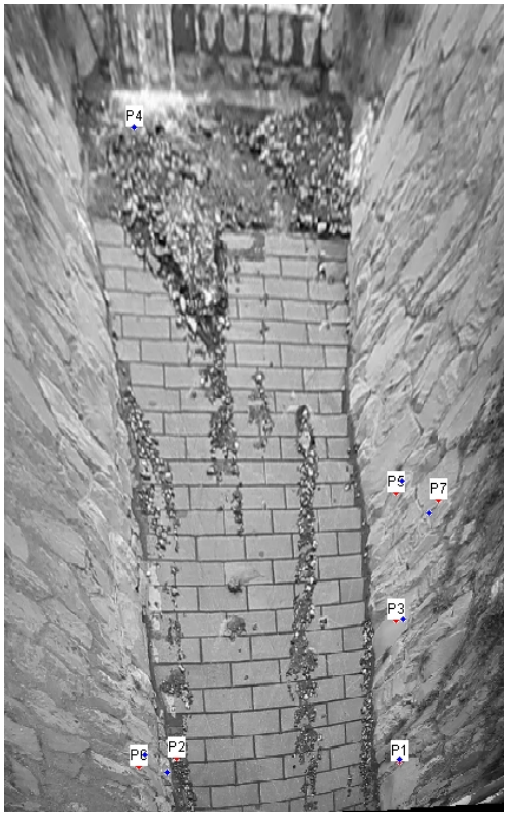

(c) Orthorectified original fisheye image

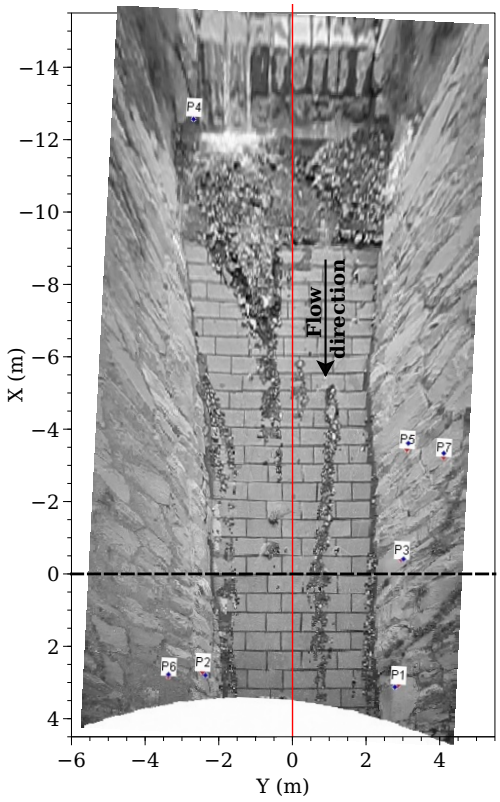

(d) Orthorectified rectilinear image. The black dash line gives the location of the reference cross-section. The red line is the torrent axis.

Figure 2: Comparison of original fisheye images and the same images corrected for distortion using rectilinear projection. The GRPs used for registration are displayed. Orthorectification is made in the plane of the torrent bottom.

Author-produced version of the article published in Hydrological Processes (2016), Volume 30, Issue 1, p 90–105
The original publication is available at http://onlinelibrary.wiley.com DOI: 10.1002/hyp.10532

all the 9 GRPs are used to compute the image orthorectification matrix. The surface velocity field and the discharge were calculated through the LSPIV process using the reference sequence (time 5:00). Then GRPs P4 and P1 were removed: they were chosen so that the resulting configuration would be the worst in terms of point alignment. Fig. 3(b) shows the obtained velocity field. Image and velocity results in both cases are very similar and the estimated discharges are 21.6 m^3/s and 21.5 m^3/s for 9 and 7 GRPs, respectively. The process therefore appears to be robust to GRP alignment. However, when the GRP P8 is also removed, even if there are still 6 GRPs remaining, the orthorectification algorithm is not able anymore to process the images correctly.

3.3 Image alignment

Home movies are commonly made with a hand-held camera, which means camera movements. In the movie of our study case, two different types of typical camera movements are present. The first movement is a coherent movement in one identified direction followed by the return to the stable position (seq. time 7:27) and the other one is a shake movement with limited amplitude and random directions (reference sequence).

Fig. 4(a) shows the time-averaged image during the first example of camera movement. For this movement, the estimated displacement in the image is ∼130 pixels in the area of the reference cross-section. The whole time-averaged image is blurred. Image alignment was then performed with Hugin using the "Align image stack" tool. It consisted in 3 steps: (1) Applying a control point detection over the image. The detector is gradient-based and produces a descriptor for each point; (2) Matching the control points in consecutive images according to their descriptor; (3) Aligning the images using these matches considered as stationary references. A time-average of the resulting images is shown in Fig. 4(b). The water flow is the only region that remains blurred, which suggests that the image alignment was correctly done. Fig. 4(e) shows the velocity component V_X in the longitudinal direction estimated at the reference cross-section as a function of the number of image pairs on which results are averaged. With image alignment, averaged velocity rapidly (∼8 image pairs) converges to a stable value. Without image alignment, the convergence requires ∼16 image pairs and the resulting velocity appears to be biased: -8.6%, -7.2% and -4.2% for 16, 30 and 50

Author-produced version of the article published in Hydrological Processes (2016), Volume 30, Issue 1, p 90–105
The original publication is available at http://onlinelibrary.wiley.com DOI: 10.1002/hyp.10532

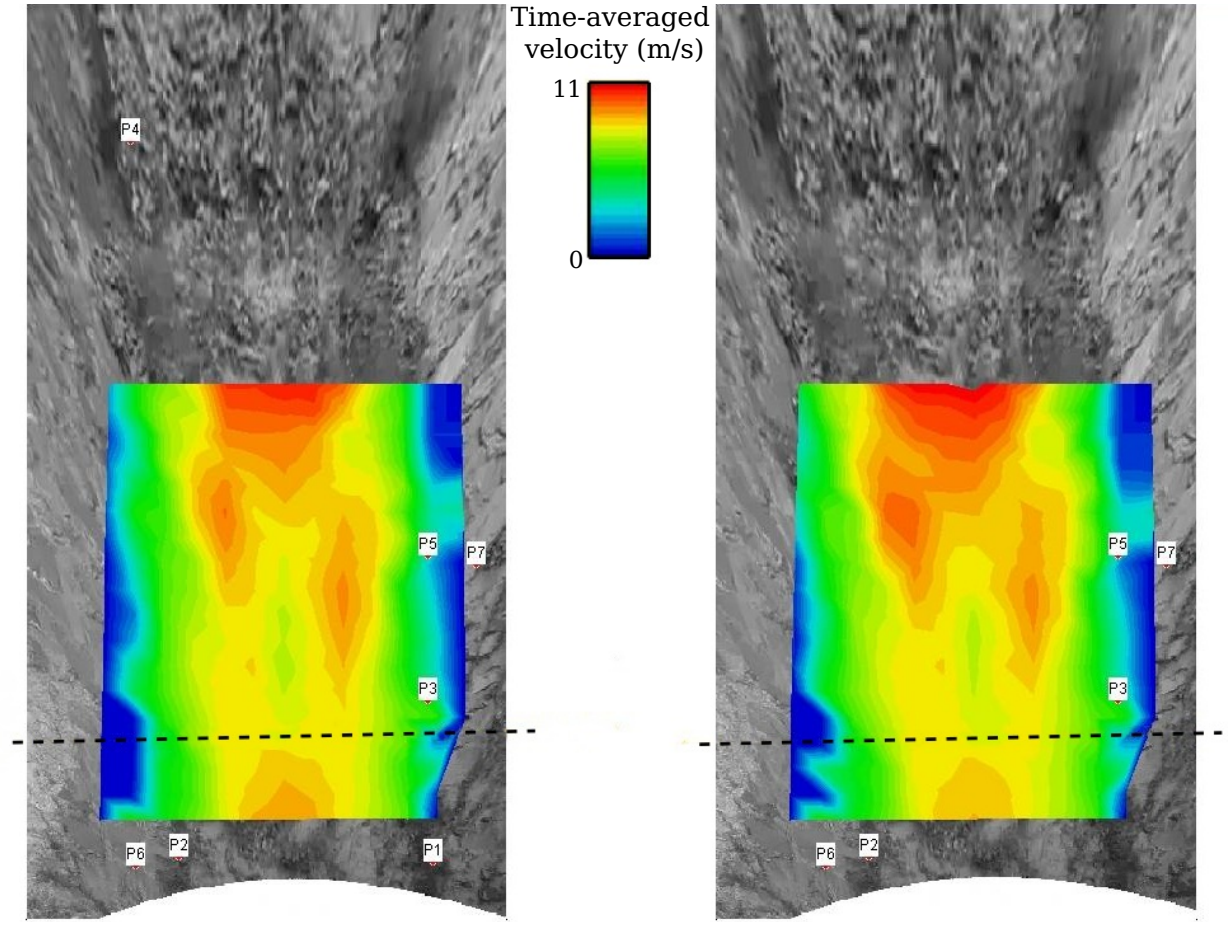

(a) (b)

Figure 3: Comparison of orthorectified images and surface velocity fields obtained using different sets of Ground Reference Points (GRPs): 9 GRPs (a) and 7 GRPs (b). GRPs P8 and P9 lie outside of the displayed orthoimage.

Author-produced version of the article published in Hydrological Processes (2016), Volume 30, Issue 1, p 90–105
The original publication is available at http://onlinelibrary.wiley.com DOI: 10.1002/hyp.10532

image pairs, respectively.

Results of the same analysis in the camera shake case are also shown in Fig. 4(cde). The movement amplitude in the area of the reference cross-section is now 4 pixels only. The blur effect in the raw average image is still present but limited. Cumulative averaged values of the longitudinal velocity with and without image alignment are given in Fig. 4(e). Very low discrepancy ($< 2\%$) is observed between the two curves. As soon as the results of $\sim$20 image pairs are averaged, the difference is negligible ($< 0.4\%$). Since the camera shake movement is random in direction and has a limited amplitude, the discrepancy in the average velocity rapidly falls to zero.

3.4 Correction of longitudinal slope

The LSPIV technique conventionally assumes that the flow free-surface is planar and the image orthorectification is made on this plane. It is also usually considered that the planar free-surface is horizontal since river slopes are generally negligible. Moreover, due to image perspective velocity vectors are more precisely estimated when images are taken from the side of the flow. The present case study faces adverse conditions because the torrent slope is steep (0.063 m/m) and the camera was placed on a bridge and aligned with the main flow direction. The example movie is typical of many situations where the flood home movie is shot longitudinally along a quite steep flow.

In the orthoimage of the dry bed, flagstones have uniform sizes when a sloped plane is considered. In turn, when a horizontal plane is considered, flagstones sizes vary from 0.9 m long in the foreground to 1.05 m long near the weir. In images with active water flow, orthorectification on a horizontal plane instead of on the sloped free-surface plane results in an overestimation of longitudinal velocities. This is illustrated in Fig. 5 that presents the longitudinal velocity component, V_X, as a function of distance X along the torrent axis, as is represented in red in Fig. 2(d). It may be observed that the discrepancy between the curves increases with distance from camera upstream of the reference cross-section. The maximum relative deviation is equal to $+22.9\%$ and is reached at $X = -5.75$ m. In the vicinity of the reference cross-section the velocity error remains low ($+5.3\%$) because the elevation of the horizontal free-surface plane was estimated at this precise location.

The slope effect depends on the viewpoint of the camera (whether it is side-looking or not) and on

Author-produced version of the article published in Hydrological Processes (2016), Volume 30, Issue 1, p 90–105
The original publication is available at http://onlinelibrary.wiley.com DOI: 10.1002/hyp.10532

(a) Time averaged image sequence

(b) Time averaged aligned image sequence

(c) Time averaged image sequence

(d) Time averaged aligned image sequence

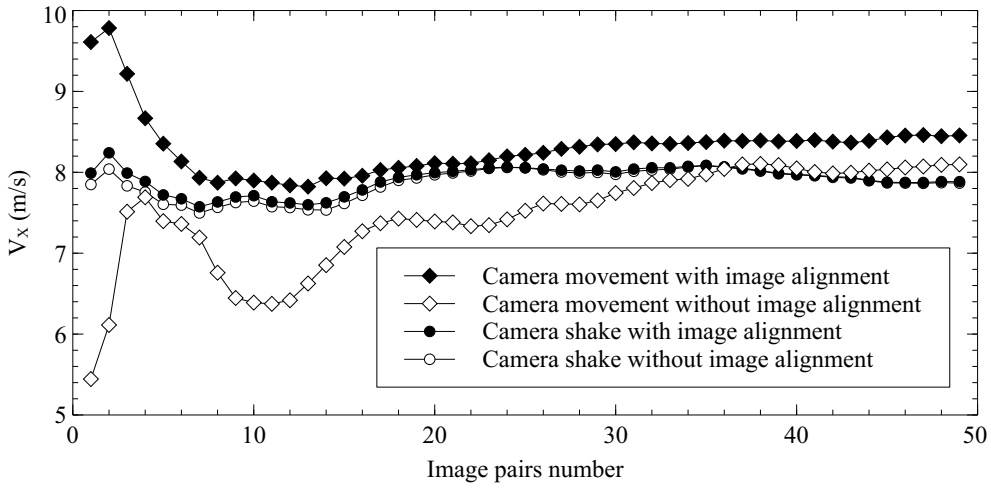

(e) Cumulative average values of streamwise velocity component, V_X, calculated at the reference cross-section with and without image alignment for the two types of movement

Figure 4: Impact of image alignment for two types of movement: **coherent** camera movement (a, b), **incoherent** (shake) camera movement (c, d), resulting LSPIV cumulative average velocity estimation (e).

Author-produced version of the article published in Hydrological Processes (2016), Volume 30, Issue 1, p 90–105
The original publication is available at http://onlinelibrary.wiley.com DOI: 10.1002/hyp.10532

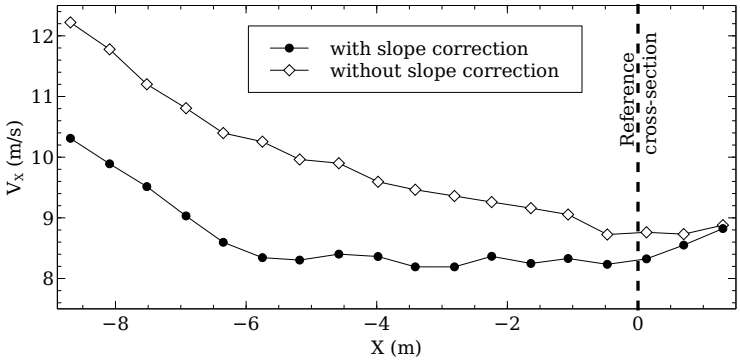

Figure 5: Impact of longitudinal slope correction on the LSPIV longitudinal velocity component, V_X, as a function of streamwise distance, X (cf. Fig. 2(d) for a representation of the X axis and the reference cross-section).

the geometry configuration relating the position of the camera, the position of the reference cross-section and the slope of the free-surface. However, in many usual cases the slope effect is negligible because free-surface slopes are lower and videos are often recorded from the river side.

3.5 Impact of the image resolution

Flood movies available in the Internet are acquired with a large diversity of sensor resolution and are often compressed to spare bandwith and storage capacity. The impact of the image resolution on velocity estimation is investigated in this section. Image resolution may indeed have an impact on two LSPIV steps: the manual selection of GRPs positions in the image and the automatic correlation-based matching.

As a typical video sharing website, YouTube enables the view of videos with different resolution levels. Fig. 6 shows the LSPIV results on the reference sequence with the different resolution options offered by YouTube. Results at resolution 720p are very similar to those obtained for the 1080p full resolution. At lowest resolutions 360p (image size 640×360 pixels) and 240p (426×240 pixels), the difference in longitudinal velocity, V_X, averaged over 50 consecutive images is less than 5% compared to full resolution. LSPIV appears to be very robust to a decrease in image resolution.

Author-produced version of the article published in Hydrological Processes (2016), Volume 30, Issue 1, p 90–105
The original publication is available at http://onlinelibrary.wiley.com DOI: 10.1002/hyp.10532

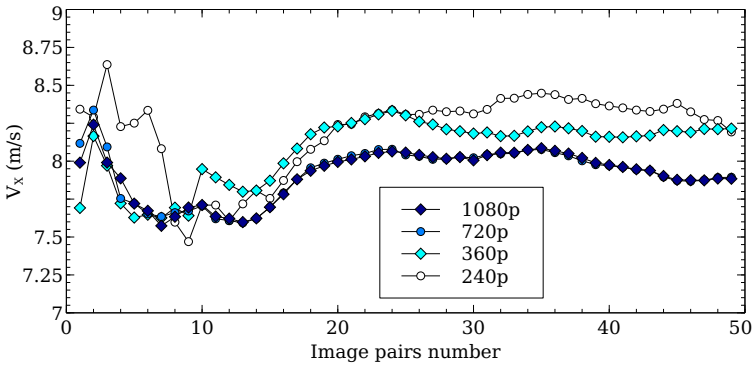

Figure 6: Impact of image resolution on the cumulative average LSPIV longitudinal velocity component, V_X, at the reference cross-section (cf. Fig. 2(d) for a representation of the X axis and the reference cross-section).

4 Application to post-flood analysis

4.1 Identification of precise location and time of image sequences

Most of the videos available in the Internet are not associated with a precise description of when and where they were recorded. The location of the video can often be deduced from the title of the file and mapping software such as Google Maps and its StreetView tool. The timing of the videos is a more difficult problem. The metadata of the videos are seldom documented and can be erroneous. The date of the recording is often mentioned, not the precise time. As an example, the movie studied in this paper was timed 1 hour too late by the author due to a confusion regarding the daylight saving time.

Contacting the authors of the collected movies is the best option to solve such problems and to get additional information. This must be done as soon as possible after the flood event so that they remember as precisely as possible the time and location of their recording. Also, authors must be contacted in order to get their personal agreement for the use and distribution of their movie materials. Finding the author of a video posted in the Internet, on YouTube for example, can be very sharp as the author is only mentioned by his user name, which is often very non-informative except for professional or semi-professional flood chasers or meteorological enthusiasts who give direct contacts.

Author-produced version of the article published in Hydrological Processes (2016), Volume 30, Issue 1, p 90–105
The original publication is available at http://onlinelibrary.wiley.com DOI: 10.1002/hyp.10532

4.2 Water level assessment

Since it is directly related to the orthorectification, velocity estimation and discharge computation, the determination of the water level simultaneously to the recording of the images is a key point of LSPIV. Videos recorded by witnesses usually do not encompass staff gauge and are not associated with direct measurements of the water stage. The water level must be therefore estimated from the recorded images and complementary topography measurements only.

The method used in this study is based on the relative positioning of the flow free-surface with stationary elements that are visible nearby the reference cross-section. One can identify in the images some characteristic objects reached by the water surface. The elevation of such objects can be measured after the flood during the topography campaign that is necessary to the GRP and cross-sectional transect positioning. During floods, the water surface is often deformed by waves created by hydraulic jumps, obstacles, roughness elements or pulsating flows. The high frequency of images acquired with conventional cameras (25 to 60 frames per second) offers a detailed sampling of waves and a good average of the free-surface elevation.

As pointed out by Dramais et al. (2011), water level errors impact the orthorectification, hence the estimation of surface velocities, as well as the computation of the wetted cross-sectional area in opposite ways, which may mutually compensate but usually lead to errors in discharge results. The sensitivity of the LSPIV process to the uncertainty on the assumed water level was tested using the reference image sequence. The water level during this sequence was estimated to be 60 cm, with an uncertainty of 15 cm based on the resolution of images and on the flow conditions. For a lower video quality, it is assumed that this uncertainty could reach 30 cm. Tab. 1 shows the results in discharge, mean velocity and wetted area obtained with different water level values 15 cm and 30 cm above and below the reference stage.

The results confirm the opposite impacts of a water level error on the velocity and area estimates. That velocity is slightly underestimated (-2%) when the stage is underestimated by 15 cm is due to modifications induced in the PIV analysis, in addition to the orthorectification error. However the area error dominates in the discharge error since discharge is systematically overestimated when the water level is overestimated. Errors in mean velocity are smaller than 3% for a 15 cm stage

Author-produced version of the article published in Hydrological Processes (2016), Volume 30, Issue 1, p 90–105
The original publication is available at http://onlinelibrary.wiley.com DOI: 10.1002/hyp.10532

Water level error (cm)	Q **(m^3/s)**	Q deviation (%)	Mean velocity V (m/s)	V deviation (%)	Wetted area A (m^2)	A deviation (%)
+30	**32.90**	+47	6.01	-5	5.47	+55
+15	**27.65**	+24	6.16	-3	4.49	+27
0	**22.36**	-	6.33	-	3.53	-
-15	**16.18**	-28	6.23	-2	2.60	-26
-30	**11.02**	-51	6.55	+3	1.68	-52

Table 1: Simulated effect of different water level errors on the discharge, mean velocity and wetted cross-sectional area. The gray box row indicates the reference computation.

bias, while the error magnitude in the wetted cross-sectional area is 27%, which approximately corresponds to the error in the final discharge value (+24% and -28% respectively). Water level is confirmed to be the dominant source of uncertainty in our study case for which the uncertainty of this parameter reaches 25%. Due to the unsteadiness of the flow, no similar test was performed for higher water levels.

4.3 Comparison with traditional methods for a quasi-steady flow

As introduced in the presentation of the studied flood event, the movie shows a pulsed flow with pseudo-periodic breaking waves overriding the base flow. To assess their agreement with the LSPIV method, traditional methods for the indirect determination of discharge were applied to the quasi-steady base flow that established between 5 successive pulses. The whole sequence lasted less than 2 min, so that the discharge was assumed to keep constant over the 5 steady state periods.

The most commonly used method is the slope-area method, which basically consists of applying the Manning-Strickler equation to the channel geometry and to the high-water marks:

$$Q = \frac{1}{n} A S^{1/2} R_h^{2/3} \tag{1}$$

with Manning's n the flow resistance coefficient, A the wetted cross-sectional area, S the longitudinal slope, R_h the hydraulic radius. Manning's n values are often derived from the table provided by

Author-produced version of the article published in Hydrological Processes (2016), Volume 30, Issue 1, p 90–105
The original publication is available at http://onlinelibrary.wiley.com DOI: 10.1002/hyp.10532

Chow (1959). In our case, we took the value proposed for "Concrete bottom float finish with sides of riprap", i.e. $n = 0.030$ [0.020-0.035].

Another way to estimate discharge is to apply the critical-depth method to the first trapezoidal weir that is visible in our images. Approximating its shape by an equivalent rectangle, the weir equation is:

$$Q = CB_s\sqrt{2g}H^{3/2} \tag{2}$$

where C is a discharge coefficient ($C \approx 0.4$), B_s is the flow width above the weir, g is the gravitational acceleration ($g = 9.81$ m/s^2), and H is the hydraulic head in the approach of the weir cross-section. Ideally, the hydraulic head should be computed as $H = D_s + V^2/(2g)$, with D_s the flow depth above the weir and V the approach velocity. However, since V estimate is usually lacking, H is sometimes abusively approximated by D_s in Eq. 2, which leads to:

$$Q = CB_s\sqrt{2g}D_s^{3/2} \tag{3}$$

Discharge estimates for the 5 quasi-steady flow sequences are presented in Tab. 2 (columns tagged "BASE FLOW"). The four methods were applied: LSPIV, slope-area (Eq. 1), and critical-depth method with (Eq. 2) and without (Eq. 3) consideration of the velocity head. All relevant variables were obtained from the geometry data and the movie analysis (cf. Tab. 3). The velocity coefficient was set at the 0.85 [0.80-0.90] default value, valid for a uniform flow over an intermediately rough bed. Note that since the water stage above the weir was very difficult to assess from images, it was roughly estimated to be 0.15 m ($\pm$0.10 m) for all pulses. Since the hydraulic control is quite sensitive to the stage, such a large uncertainty in stage leads to a wide uncertainty interval, from 0.1 to 1 m^3/s.

For this base flow, the LSPIV and slope-area (Eq. 1) methods yielded consistent discharge estimates (+7.7%), considering the uncertainty in the LSPIV velocity coefficient and in the Manning's n coefficient, respectively. The results actually suggest that the base flow was actually not constant and significantly decreased over the pulse series, from 3.7 m^3/s to 1.3 m^3/s (LSPIV values). As could be expected, the velocity head dominates the total hydraulic head and when ignoring it, the critical-depth method (Eq. 3) severely underestimates the discharge. When correctly applied using

Author-produced version of the article published in Hydrological Processes (2016), Volume 30, Issue 1, p 90–105
The original publication is available at http://onlinelibrary.wiley.com DOI: 10.1002/hyp.10532

LSPIV-derived velocities, the critical-depth method (Eq. 2) significantly overestimates the LSPIV discharge (by 65%). This may be because we used the velocities measured downstream of the weir, which are potentially higher than the actual approach velocity upstream of the weir, where LSPIV application is not practicable. The main issue for applying the critical-depth method remains that velocity measurements are usually not available to compute the hydraulic head accurately.

4.4 Pulsed flow and time-averaged discharge estimate

The issue of determining the discharge of pulsed flows was first introduced by Holmes (1936). Heggen (1986) pointed out the fact that 'Post-event surveys of floods in surged channels is likely to yield overestimates of discharge if high-water marks and displaced bed material are assumed to be representative of peak uniform-flow conditions'. The same author summarized state-of-the-art formulas for describing the height, shape, wavelength and velocity of the periodic surges created in pulsating flows.

A simple method for computing the time-average discharge, $\overline{Q}$, of a pulsating flow in a channel of width B is to separately consider the time-average discharge, Q_w, of the overriding translatory wave flow, and that, Q_1, of the base flow. Assuming that the latter base flow is quasi-steady and uniform and that the wave shape can be approximated as a triangle wedge, Thompson (1968) (see also WMO, 2010, chapter 8.7) proposed the following equation (cf. Fig. 7(a) for a definition of the variables):

$$\overline{Q} = Q_1 + Q_w = V_1 D_1 B \; + \; \frac{h_w L_w B}{2\, T_p} \tag{4}$$

Using this method, Thompson (1968) obtained acceptably accurate results from controlled tests in a concrete-lined, rectangular, flood control channel. However, it should be noted that the solution technique provided by Thompson (1968) is simplified since based on a geometrical approximation taken for the wave shape, and originally evaluated against measurements of uncertain quality. According to Brock's experiments (1967, 1968, 1970) reported by Richard and Gavrilyuk (2012), the actual profile of roll waves is composed of three segments: a vertical front followed by a progressive rise to the wave peak, then a slightly concave falling limb (cf. Fig. 7a). Richard and Gavrilyuk (2012) recently introduced a model based on a sounder description of the physical processes and

Author-produced version of the article published in Hydrological Processes (2016), Volume 30, Issue 1, p 90–105
The original publication is available at http://onlinelibrary.wiley.com DOI: 10.1002/hyp.10532

accurately reproduced the actual shape of roll waves reported from Brock's experiments. However, refining the shape of waves using such complex models would not significantly improve discharge estimates from flood home movies, due to the uncertainty in estimated water levels as reported in Section 4.2. Typically, a more significant improvement in the estimation of mean discharge can be expected from the accurate evaluation of pseudo-periods between pulses. Therefore, a simple method derived from Thompson's works seems to be efficient for flood discharge estimation purpose, even if in most favourable conditions it might be valuably refined according to most recent advances on the roll wave dynamics.

Considering that the LSPIV application directly provides us with discharge estimates during base flow, Q_1, and during the pulse front, Q_2, a similar time-averaging equation can be established as follows (cf. Fig. 7(b)):

$$\overline{Q} = \frac{1}{T_p}\left[(T_p - t_b)\,Q_1 + t_b\,\frac{Q_1 + Q_2}{2}\right] \tag{5}$$

Setting the velocity coefficient in the pulse wave is problematic because the velocity distribution inside such a transient flow is highly uncertain. As a simple approximation, we chose to keep the velocity coefficient equal to 0.85 in the overrun flow and to 1 in the overriding flow layer, assuming that the velocity is roughly homogeneous within the breaking wave. That means that V_w is taken equal to the surface velocity yielded by the LSPIV and that the maximum surge discharge is computed as $Q_2 = V_w B\,[0.85D_1 + (D_2 - D_1)]$.

The analysis of the St-Julien flood movie allows for applying both time-averaging equations for a series of successive pulses. The same sequence of 5 successive surges was investigated in order to estimate the geometrical properties and the velocities of the overriding waves and base flow (cf. Tab. 3). The time period between the arrivals of consecutive wave fronts, T_p, was easily derived from the video sequence and was found to be quite stable and close to 23 s on average. The two last pulses show slighty longer periods and lower velocities. Similarly, the time interval, t_b, between the front and the tail of the surges was recorded and found to be 15 s on average. The length of the surge wedges was then computed as $L_w = V_w t_b$.

The flow depths, D_1 and D_2, were estimated using the method already presented in Section 4.2, with the same level of uncertainty. The surge ratio, D_2/D_1 was found to be as high as 7 on average.

Author-produced version of the article published in Hydrological Processes (2016), Volume 30, Issue 1, p 90–105
The original publication is available at http://onlinelibrary.wiley.com DOI: 10.1002/hyp.10532

While Heggen (1986) explained that there is no absolute maximum for breaking waves such as those observed here, the D_2/D_1 ratio is actually much higher than the upper bound he suggests, i.e. 2. The LSPIV analysis also provided direct estimation of velocities, V_1 and V_w, which were not available to Thompson (1968) typically. The wave velocities obtained using LSPIV were found to be in reasonable agreement with robust visual checks by tracking visible floating objects (cf. Tab. 3). The observed velocity ratio, $V_w/V_1 = 2.41$, is again much higher than what suggests the theoretical relation reported by Heggen (1986), that yields $V_w/V_1 = 1.67$ for a wide channel, and even lower for a narrow trapezoidal channel such as ours. It subsequently appears that the recorded pulses were more severe than was reported in previous studies.

Tab. 2 summarizes the discharge estimates provided by all tested methods for the base flow (Q_1), pulse flow (Q_2) and time-average flow ($\overline{Q}$) over the series of 5 pulses. The same decreasing trend is observed for Q_2 and $\overline{Q}$ as for Q_1, except for the fourth pulse which was the strongest in the series. From LSPIV data, the ensemble-averaged discharges of the base flow, pulse flow and time-averaged flow were found to be 2.6 m^3/s, 62.8 m^3/s and 22.1 m^3/s, respectively. The discrepancy between such values illustrate the highly transient nature of such a flow that cannot be captured by traditional high-water mark surveys. As was the case for base flow, the slope-area method (Eq. 1) produced consistent, though slightly overestimated (+17.5%) estimates of the pulse flow discharge compared to the LSPIV reference, while the critical-depth method now underestimates the discharge by −75% when the velocity head is not accounted for (Eq. 3), and by −59% when it is (Eq. 2). This may be explained by the non-ideal flow conditions upstream of the weir, especially the unsteadiness of the wave flow and the very high approach velocity.

As mentioned by Holmes (1936) and Heggen (1986), when direct observations of a pulsating flow are missing, the pulsed nature of the flow may often be ignored. Then, a typical mistake would be to estimate discharge by applying the slope-area method to the high-water marks with the underlying steady, uniform flow assumption. As expected, the slope-area method (Eq. 1) applied with D_2 as the flow depth would fail in providing a realistic time-averaged discharge, $\overline{Q}$, which would be severely overestimated (73.8 m^3/s, instead of 22.1 m^3/s). As also expected, both Eq. 4 and Eq. 5 provide very similar ensemble-averaged estimates of $\overline{Q}$ (22.2 m^3/s and 22.1 m^3/s, respectively). Similar results are obtained when equations are directly applied to the mean parameter values (21.8 m^3/s

Author-produced version of the article published in Hydrological Processes (2016), Volume 30, Issue 1, p 90–105
The original publication is available at http://onlinelibrary.wiley.com DOI: 10.1002/hyp.10532

and 22.4 m^3/s, respectively, not shown in Tab. 2).

5 Conclusions and perspectives

The selected example of a pulsed flash-flood flow recorded in Saint-Julien torrent illustrates the typical issues and interests of flood home movies taken by witnesses for improving post-flood discharge estimation. In spite of non-ideal conditions related to such movies, the Large Scale Particle Image Velocimetry (LSPIV) technique was successfully applied using user-friendly, free software only, such as Fudaa-LSPIV. Corrections for lens distortion (fisheye) and camera movements are not difficult to apply and can reduce the related errors to a few percents. They may not always be necessary, especially when the area of interest is located at the image center and when camera movement is limited and incoherent over the sequence (camera shake). The lowest resolution levels offered by YouTube did not produce differences in time-averaged longitudinal velocity greater than 5% compared to the results from full resolution image sequences, which suggests that image resolution is usually not a problem if not extremely poor. Orthorectification is more easily possible in urban areas where fixed Ground Reference Points (GRP) are visible at both sides of the flow. A limited number of GRPs, typically 10, is required but they must be adequately distributed around the area of interest.

Locating precisely the video viewpoint is often easy whereas precise timing may be not, especially when the author of the video cannot be contacted. The indirect determination of the water level is the main source of uncertainty in the results, usually much more than errors due to the longitudinal slope of the flow free-surface and likely more than errors due to its waviness. The image-based method yielded direct discharge estimates of the base flow between pulses, of the pulse waves, and of the time-averaged flow over a movie sequence. A comparison with traditional indirect determination methods showed that the critical depth method may produce significantly biased results for such a fast, unsteady flow with very uncertain approach velocity, while the slope-area method seems to be more robust but would overestimate the time-average flow rate if applied to the high-water marks of a pulsed flow.

We think that this application case covers all the major practical issues related to usable flood home movies but one, namely bed changes during the flood. The solutions applied and discussed

Author-produced version of the article published in Hydrological Processes (2016), Volume 30, Issue 1, p 90–105
The original publication is available at http://onlinelibrary.wiley.com DOI: 10.1002/hyp.10532

in the paper are fully reproducible and are not site-specific. However, we highlight which situations may be detrimental to their successful application, such as the absence or lack of GRPs in fully natural environments. The ranking of error sources and limitations is deemed to be valid for most situations, based on our experience on several other cases.

This work also calls for further developments of the technique to extend it to more difficult flood home movies available in video sharing platforms and other sources. Implementing other image velocimetry techniques such as STIV or optical flow is an interesting perspective to enhance the robustness and versatility of the method. Stereo-photogrammetry could be a promising solution to the important issue of GRP availability: Though common people only use one camera, trained observers could use a calibrated system with two cameras. In the same vein, the issue of bed changes could be tackled with non-intrusive bathymetry measurements, or some inference of bathymetry changes from the comparison with numerical hydraulic simulations. Such ambitious developments should be eventually tested and validated in experiments under controlled conditions.

The analysis of flood movies offers a direct insight in flow processes and potentially answers to important issues for post-flood analyses. First, it provides direct measurements of the surface flow velocities, which are usually unknown. It is interesting to note that several flood movies, such as the one used to support this study, provided velocity estimates that significantly exceed the velocity magnitudes commonly accepted as realistic in such extreme events. Typically, maximum velocities greater than 10 m/s and 7 m/s were observed in torrents and rivers, respectively, where 7 m/s and 4 m/s at most, respectively, would have been expected.

Second, the movies offer the direct observation of the flow conditions, which helps in assessing the applicability and uncertainty of the applied hydraulic formulas and models. The knowledge of the approach velocity upstream of a critical section and of the head losses homogeneity along the control channel are key for the application of the critical-depth method and of the slope-area method, respectively. The movies may also provide pictures of obstacles, log jams, pulsating flows, hydraulic jumps, and other complex hydraulic processes, especially in urban areas, that have a strong influence on the high-water marks.

Last, the abundance of movies recorded by different people provides information at different locations of the river catchment and at different moments of the flood event. Such synoptic results, even

Author-produced version of the article published in Hydrological Processes (2016), Volume 30, Issue 1, p 90–105
The original publication is available at http://onlinelibrary.wiley.com DOI: 10.1002/hyp.10532

if they are discontinuous and non simultaneous, are very valuable for reconstructing the dynamics of the flood processes at the relevant spatio-temporal scale. The proposed method therefore appears as a promising way to make flood studies more collaborative and more comprehensive thanks to the participation of volunteers amongst the men in the street, or more accurately amongst the men by the river. Typically, to encourage the production of valuable flood home movies simple recommendations and field procedures were proposed as part of the FloodScale research project on Mediterranean flash-floods. The document was shared with local stakeholders and inhabitants and is available online[5]. Priority on safety rules is emphasized in the document: recording flood movies can be dangerous. Never risk your life for flood data.

Acknowledgements

This work was supported by the French national hydrological services (SCHAPI). The FloodScale project is funded by the French National Research Agency (ANR) under Contract No ANR 2011 BS56 027, which contributes to the HyMeX program. We are grateful to Alexandre Modesto who, as a flood chaser, provided us with the movie material of this study, to Mickaël Lagouy (Irstea) who conducted the complementary field measurements, and to Magali Jodeau (EDF) who leads the co-development of the Fudaa-LSPIV free software by EDF and Irstea. We appreciated the valuable comments from Prof. Marco Borga (University of Padova, Italy) and two other anonymous reviewers.

References

Adrian, R. J. (1991). Particle-imaging techniques for experimental fluid mechanics. *Annu. Rev. Fluid Mech.*, 23:261–304. 5

Bonnifait, L., Delrieu, G., Le Lay, M., Boudevillain, B., Masson, A., Belleudy, P., Gaume, E., and Saulnier, G.-M. (2009). Distributed hydrologic and hydraulic modelling with radar rainfall input:

[5] http://floodscale.irstea.fr/

Reconstruction of the 8-9 September 2002 catastrophic flood event in the Gard region, France. *Advances in Water Resources*, 32:1077–1089. 4

Borga, M., Gaume, E., Creutin, D., and Marchi, L. (2008). Surveying flash floods: gauging the ungauged extremes. *Hydrological processes*, 22:3883–3885. 3

Chow, V.T. (1959). Open-Channel Hydraulics. McGraw-Hill, New York, 680 pp. ISBN 1-9328461-8-2. 23

Creutin, J. D., Muste, M., Bradley, A. A., Kim, S. C., Kruger, A. (2003). River gauging using PIV techniques: a proof of concept experiment on the Iowa river. *Journal of Hydrology*, 277:182–194. 5

Delrieu, G., Ducrocq, V., Gaume, E., Nicol, J., Payrastre, O., Yates, E., Kirstetter, P. E., Andrieu, H., Ayral, P. A., Bouvier, C., Creutin, J. D., Livet, M., Anquetin, S., Lang, M., Neppel, L., Obled, C., du Chatelet, J. P., Saulnier, G. M., Walpersdorf, A., Wobrock., W. (2005). The catastrophic flash-flood event of 8-9 september 2002 in the Gard region, France: a first case study for the Cévennes-Vivarais Mediterranean Hydro-meteorological Observatory. *Journal of Hydrometeorology*, 6:34–52. 4

Dramais, G., Le Coz, J., Camenen, B., and Hauet, A. (2011). Advantages of a mobile LSPIV method for measuring flood discharges and improving stage-discharge curves. *Journal of Hydro-Environmental Research*, 5(4):301–312, 2011. 5, 6, 7, 9, 21

Fujita, I., Muste, M., and Kruger, A. (1998). Large-scale particle image velocimetry for flow analysis in hydraulic engineering applications. *Journal of Hydraulic Research*, 36(3):397–414. 5

Fujita, I. and Hino, T. (2003). Unseeded and seeded PIV measurements of river flows videotaped from a helicopter. *Journal of Visualization*, 6(3):245–252. 5

Fujita, I., Watanabe, H. and Tsubaki, R. (2007). Development of a non-intrusive and efficient flow monitoring technique: The space time image velocimetry (STIV). *International Journal of River Basin Management*, 5(2):105–114. 5

Fujita, I. and Kunita, Y. (2011). Application of aerial LSPIV to the 2002 flood of the Yodo River using a helicopter mounted high density video camera. *Journal of Hydro-environment Research*, 5(4):323–331. 5

Fujita, I., Kunita, Y., and Tsubaki, R. (2013). Image analysis and reconstruction of the 2008 Toga River Flash Flood in an urbanised area. *Australian Journal of Water Resources*, 16(2), 12 p.

Gaume, E., Livet, M., Desbordes, M., and Villeneuve, J.-P. (2004). Hydrological analysis of the river Aude, France, flash flood on 12 and 13 November 1999. *Journal of Hydrology*, 286:135–154. 3

Gaume, E., and Borga, M. (2008). Post flood field investigations after major flash floods: proposal of a methodology and illustrations. *Journal of flood risk management*, 1:175–189. 4

Hauet, A., Kruger, A., Krajewski, W., Bradley, A., Muste, M., Creutin, J., and Wilson, M. (2008a). Experimental system for real-time discharge estimation using an image-based method. *Journal of Hydrologic Engineering*, 13(2):105–110. 5

Hauet, A., Creutin, J.-D., Belleudy, P. (2008b). Sensitivity study of large-scale particle image velocimetry measurement of river discharge using numerical simulation. *Journal of Hydrology*, 349(1-2):178–190. 6

Heggen, R. (1986). Periodic surges and sediment mobilization. *IAHS-AISH publication*, 159:323-333. 24, 26

Holmes, W.H. (1936). Traveling waves in steep channels. *Civil Eng.*, 6(7):467-468. 24, 26

Jarrett, R.D. (1987). Errors in slope-area computations of peak discharges in mountain streams. *Journal of Hydrology*, 96(1-4):53–67. 3

Jodeau, M., Hauet, A., Paquier, A., Le Coz, J., Dramais, G. (2008). Application and evaluation of LS-PIV technique for the monitoring of river surface velocities in high flow conditions. *Flow Measurement and Instrumentation*, 19(2), 117–127. 5

Kim, Y., Muste, M., Hauet, A., Krajewski, W. F., Kruger, A., Bradley, A. (2008). Stream discharge using mobile large-scale particle image velocimetry: A proof of concept. *Water Resources Research*, 44, W09502. 5

Kirby, W.H. (1987). Linear error analysis of slope-area discharge determinations. *Journal of Hydrology*, 96(1-4):125–138. 3

Le Coz, J., Hauet, A., Dramais, G., and Pierrefeu, G. (2010). Performance of image-based velocimetry (LSPIV) applied to flash-flood discharge measurements in Mediterranean rivers. *Journal of Hydrology*, 394:42–52. 5, 6, 13

Le Coz, J., Jodeau, M., Hauet, A., Marchand, B., and Le Boursicaud, R. (2014). Image-based velocity and discharge measurements in field and laboratory river engineering studies using the free Fudaa-LSPIV software. *Proceedings of the International Conference on Fluvial Hydraulics, RIVER FLOW 2014*, 1961–1967. 5, 11, 13

Lloyd, P. M., Ball, D. J., and Stansby, P. K (1995). Unsteady surface-velocity field measurement using particle tracking velocimetry. *Journal of Hydraulic Research*, 33(4):519–534. 5

Lumbroso, D., and Gaume, E. (2012). Reducing the uncertainty in indirect estimates of extreme flash flood discharges. *Journal of Hydrology*, 414–415:16–30. 3, 4

Maybank, S.J. and Faugeras, O.D. (1992). A theory of self-calibration of a moving camera. *International Journal of Computer Vision*, 8(2):123–151. 7

Muste, M., Fujita, I., and Hauet, A. (2008). Large-scale particle image velocimetry for measurements in riverine environments. *Water Resour. Res.*, 44, W00D19, doi:10.1029/2008WR006950. 6

Muste, M. and Fujita, I. and Hauet, A. (2010) Large-scale particle image velocimetry for measurements in riverine environments. *Water Resources Research*, 46(4):123–151. 13

Muste, M., Ho, H.-C., and Kim, D. (2011) Considerations on direct stream flow measurements using video imagery: Outlook and research needs. *Journal of Hydro-environment Research*, 5: 289–300, 2011. 5

Perkins, R.J., and Hunt, J.C.R. (1989). Particle tracking in turbulent flows. *Advances in turbulence*, 2:286–291. 5

Pollefeys, M. and Van Gool, L. and Vergauwen, M. and Verbiest, F. and Cornelis, K. and Tops, J. and Koch, R. (2004). Visual modeling with a hand-held camera. *International Journal of Computer Vision*, 59(3):207–232. 7

Richard, G. L. and Gavrilyuk, S. L. (2012). A new model of roll waves: comparison with Brock's experiments. *J. Fluid Mech.*, 698:374–405. 24, 35

Thompson, R.T. (1968). Determination of discharge during pulsating flow. *U.S. Geol. Survey*, Water-Supply Paper 1869-D, 22 p. 24, 26, 35

Tsubaki, R., Fujita, I., and Tsutsumi, S. (2011). Measurement of the flood discharge of a small-sized river using an existing digital video recording system. *Journal of Hydro-environment Research*, 5(4):313–321. 5

World Meteorological Organization (2010). Manual on Stream Gauging. Volume I – Fieldwork *WMO-No. 1044*, 250 p. 3, 24

		BASE FLOW (Q_1)				PULSE FLOW (Q_2)				TIME-AVERAGE ($\overline{Q}$)	
Pulse order	time (min:sec)	**LSPIV*** **(m^3/s)**	Eq. 1 (m^3/s)	Eq. 3** (m^3/s)	Eq. 2** (m^3/s)	**LSPIV*** **(m^3/s)**	Eq. 1 (m^3/s)	Eq. 3 (m^3/s)	Eq. 2 (m^3/s)	Eq. 4 (m^3/s)	**Eq. 5** **(m^3/s)**
P1	07:10	**3.7**	4.2	0.5	4.2	**71.9**	91.2	28.7	42.7	28.4	**25.8**
P2	07:31	**3.4**	2.9	0.5	7.4	**65.7**	67.2	6.4	19.7	22.4	**24.6**
P3	07:51	**2.5**	2.2	0.5	4.5	**53.8**	54.4	10.0	19.7	18.6	**19.2**
P4	08:12	**2.5**	2.9	0.5	3.6	**79.1**	101.7	24.7	36.0	28.6	**27.2**
P5	08:38	**1.3**	1.8	0.5	1.6	**43.6**	54.4	9.8	12.9	13.2	**14.0**
mean		**2.6**	2.8	0.5	4.3	**62.8**	73.8	15.9	26.2	22.2	**22.1**
std		**0.8**	0.8	0.0	1.9	**12.7**	19.4	9.0	11.2	5.9	**4.9**
std/mean		**32%**	29%	0%	44%	**20%**	26%	56%	43%	26%	**22%**

Table 2: Discharges estimated over 5 successive pulses recorded in the Saint-Julien torrent flood movie. Q_1, Q_2 and $\overline{Q}$ are the discharges of the base flow between pulses, of the pulse flow and of the time-average flow, respectively. Eq. 1 refers to the slope-area method, while Eq. 2 and Eq. 3 refer to critical-depth methods with and without considering the velocity head, respectively. Eq. 4 and Eq. 5 are two different methods for time-averaging the LSPIV-derived base and pulse flows (cf. text). Bold numbers are the best LSPIV-based discharge estimates.

*: In LSPIV discharge computation, velocity coefficients were assumed to be 0.85 for base flow and 1 within the pulse flow.

**: For base flow, the water stage above the weir is very difficult to assess from images; It was therefore roughly estimated to be 0.15 m ($\pm$0.10 m) for all pulses.

Author-produced version of the article published in Hydrological Processes (2016), Volume 30, Issue 1, p 90–105
The original publication is available at http://onlinelibrary.wiley.com DOI: 10.1002/hyp.10532

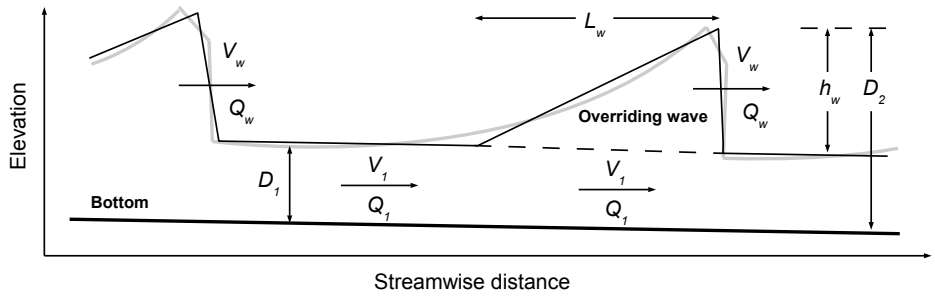

(a)

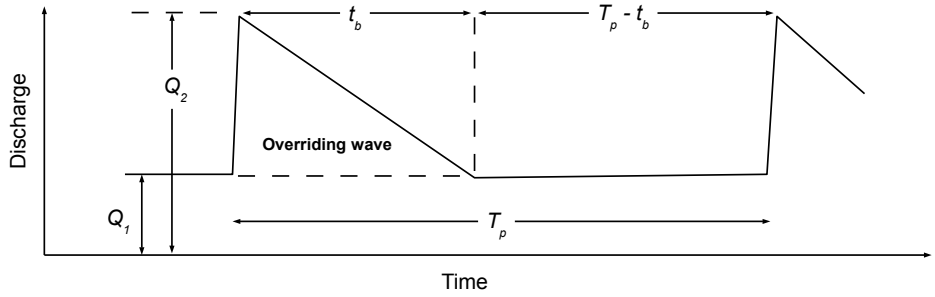

(b)

Figure 7: Schematic longitudinal elevation profile (a, modified after Thompson, 1968) and discharge time series (b) of a pulsated flow showing all useful variables for time-averaged discharge estimation. A more realistic profile of the roll waves is plotted in light gray (a, according to Brock's experiments reported by Richard and Gavrilyuk, 2012). D_1, V_1, Q_1, are the depth, velocity, discharge, respectively, of the base flow. L_w, h_w, V_w, Q_w, are the length, height, mean velocity, mean discharge, respectively, of the surge. T_p is the time period between pulses, and t_b the transit time of pulse waves. The total flow depth at surge fronts, D_2, is equal to $D_1 + h_w$. The total discharge at surge fronts, Q_2, is considered over the full flow depth.

Author-produced version of the article published in Hydrological Processes (2016), Volume 30, Issue 1, p 90–105
The original publication is available at http://onlinelibrary.wiley.com DOI: 10.1002/hyp.10532

Pulse order	time (min:sec)	D_1 (m)	D_2 (m)	D_2/D_1 (-)	T_p (s)	t_b (s)	B (m)	D_s (m)	V_1 (m/s)	V_w^* (m/s)	V_w^{**} (m/s)
P1	07:10	0.25	1.55	6.2	21	14	8.0	1.6	3.1	7.1	7.8
P2	07:31	0.20	1.30	6.5	20	14	6.2	0.7	3.9	8.0	6.6
P3	07:51	0.17	1.15	6.8	21	14	6.6	0.9	3.2	7.5	7.8
P4	08:12	0.20	1.65	8.3	26	17	7.6	1.5	2.9	7.2	7.2
P5	08:38	0.15	1.15	7.7	28	17	6.5	0.9	1.9	6.1	9.1
mean		0.19	1.36	7.1	23	15	7.0	1.1	3.0	7.2	7.7
std		0.03	0.21	0.8	3	1	0.7	0.4	0.7	0.6	0.8
std/mean		17%	15%	11%	14%	10%	10%	32%	22%	9%	11%

Table 3: Flow characteristics observed over 5 successive pulses recorded in the Saint-Julien torrent flood movie. See Fig. 7 and text for definition of variables. Velocities V_1 and V_w^* were measured using LSPIV with 0.85 and 1 as velocity coefficients, respectively. V_w^{**} is a visual check by tracking visible floating objects.